

# Orbital Dimerization and Dynamic Jahn-Teller Effect in $\text{NaTiSi}_2\text{O}_6$

M. J. Konstantinović <sup>a,\*</sup>, J. van den Brink, <sup>b</sup> Z. V. Popović <sup>a,c,\*\*</sup>, V. V. Moshchalkov <sup>a</sup>, M. Isobe <sup>d</sup>, and Y. Ueda <sup>d</sup>

<sup>a</sup> *Laboratorium voor Vaste-Stoffysica en Magnetisme,*

*Katholieke Universiteit Leuven, Celestijnenlaan 200D, B-3001 Leuven, Belgium*

<sup>b</sup> *Institut-Lorentz for Theoretical Physics, Universiteit Leiden,*

*P.O. Box 9506, 2300 RA Leiden and Faculty of Applied Physics,*

*University of Twente, P.O. Box 217, 7500 AE Enschede, The Netherlands*

<sup>c</sup> *Institute of Physics-Belgrade, P. O. Box 68, 11080 Belgrade/Zemun, Yugoslavia and*

<sup>d</sup> *Institute for Solid State Physics, The University of Tokyo,*

*5-1-5 Kashiwanoha, Kashiwa, Chiba 277-8581, Japan*

We study with Raman scattering technique two types of phase transitions in the pyroxene compounds  $\text{NaMSi}_2\text{O}_6$  (with  $M=\text{Ti}$ ,  $\text{V}$ , and  $\text{Cr}$ ). In the quasi one-dimensional  $S=1/2$  system  $\text{NaTiSi}_2\text{O}_6$  we observe anomalous high-temperature phonon broadening and large changes of the phonon energies and line-widths across the phase transition at 210 K. The phonon anomalies originate from an orbital order-disorder phase transition and these results –combined with theoretical considerations– indicate that the high temperature dynamical Jahn-Teller phase of  $\text{NaTiSi}_2\text{O}_6$  exhibits a spontaneous breaking of translational symmetry into a dimerized, Jahn-Teller distorted, orbital ordered state under the formation of spin valence bonds. In  $S=1$   $\text{NaVSi}_2\text{O}_6$  orbital degrees of freedom are strongly suppressed and the magnetic excitations are well described within a Heisenberg model, indicating that at  $T_N=19\text{K}$  this system orders antiferromagnetically.

PACS numbers: 78.30.-j, 75.50.Ee, 75.30.Et, 71.21.+a

*Introduction.* Electrons in strongly correlated transition-metal compounds can be regarded as having separate spin, charge and orbital degrees of freedom. It is the interplay between these, combined with their coupling to the lattice, that gives rise to a wealth of possible spin, charge and orbital orderings, as observed for instance in many Colossal Magneto-Resistance manganites [1], cuprates [2], titanates (e.g.  $\text{LaTiO}_3$  [3]) and vanadates (e.g.  $\text{V}_2\text{O}_3$  [4] and  $\text{LiVO}_2$  [5]). Also the low-energy elementary excitations –responsible for the rich variety of physical phenomena that are encountered in these materials– are characterized by the complex interplay of these different degrees of freedom.

Systems with orbital degeneracy are particularly interesting because orbitals couple to the lattice via the cooperative Jahn-Teller (JT) effect on one hand, and via superexchange interactions to the electronic spin on the other hand [2]. Therefore at an orbital ordering phase transition the magnetic susceptibility and phonon properties will be affected at the same time. Experimentally, however, such an interrelation is seldom found: in general the dominant JT orbital-lattice coupling obscures the more subtle effects due to the superexchange.

In this Letter, we report a Raman scattering study on a family of pyroxene compounds from which we conclude that  $\text{NaTiSi}_2\text{O}_6$  undergoes an orbital order phase transition at  $T_{\text{OO}}=210\text{ K}$ . At high temperatures the fluctuations of the orbital degrees of freedom lead to a dynamic Jahn-Teller phase with anomalous phonon broadening and remnant antiferromagnetic (AF) spin fluctuations. We find that the dramatic drop of the magnetic susceptibility below  $T_{\text{OO}}$  is accompanied with a structural change, just as one would expect for a canonical orbital ordering transition. These results, combined

with the microscopic orbital-spin model that we derive, suggest that the quasi one-dimensional dynamical Jahn-Teller phase of  $\text{NaTiSi}_2\text{O}_6$  exhibits a spontaneous breaking of the translational symmetry into an dimerized orbital ordered state with a spin gap due to the formation of spin valence bonds.

*Pyroxenes: experimental.* Studies on the pyroxene family of compounds ( $\text{AMB}_2\text{O}_6$ ;  $A=\text{alkali-metal}$ ,  $M=\text{transition-metal}$ , and  $B=\text{Si, Ge}$ ) indicate that almost all systems in this class of materials show AF ordering at low temperatures [6, 7, 8, 9]. The structure of pyroxenes consists of isolated quasi one-dimensional chains of edge-sharing  $\text{MO}_6$  octahedra, linked together by the corner-sharing  $\text{BO}_4$  tetrahedra, see Fig. 1. The sodium-silicon system with titanium,  $\text{NaTiSi}_2\text{O}_6$ , however, is rather different from the other pyroxenes as it lacks low-temperature antiferromagnetic order and shows signs of the opening of a spin gap instead.  $\text{Ti}^{3+}$  corresponds to  $S=1/2$ , and since all Ti ions are in equivalent crystallographic positions, this material is a prime candidate to show a spin-Peierls (SP) phase transition. Indeed, its magnetic susceptibility [6] sharply decreases below 210 K, indicating a transition to a spin-singlet state, which could in principle be of the SP type. But already the high-temperature magnetic susceptibility data does not support such a SP scenario, since the phase transition occurs at a temperature that is higher than the maximum point of the Bonner-Fisher curve, which implies that the transition cannot solely be driven by magnetic fluctuations [6]. From the present Raman study and the theoretical considerations we reach the conclusion that this phase transition is in fact driven by orbital ordering.

High-quality powder samples of  $\text{NaMSi}_2\text{O}_6$  ( $M=\text{Ti}$ ,  $\text{V}$ , and  $\text{Cr}$ ) were prepared by a solid-state reaction of mix-

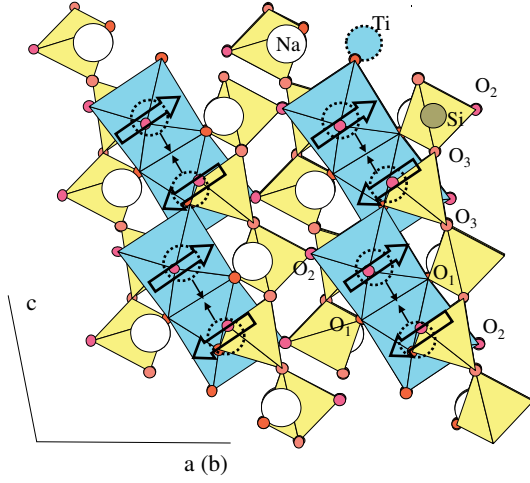


FIG. 1: a) Crystal structure of  $\text{NaTiSi}_2\text{O}_6$ . Block arrows denote magnetic moments, and small arrows represent possible distortions (dimerization) of the  $\text{TiO}_6$  octahedra in the low temperature phase.

tures with an appropriate molar ratio of  $\text{Na}_2\text{MSi}_4\text{O}_{11}$ , M and  $\text{MO}_2$ . Details of the sample preparation are published elsewhere [6]. Raman spectra are measured in the backscattering configuration, using 514.5 nm line of an Ar-ion laser, micro-Raman system with a DILOR triple monochromator, and a liquid nitrogen cooled charge-coupled device detector. For the low-temperature measurements we used the Oxford continuous-flow cryostat with a 0.5 mm thick window. The focusing of the laser beam is realized with a long distance (10 mm focal length) microscope objective (magnification  $50\times$ ).

The pyroxenes crystallize in a monoclinic unit cell with the space group  $C2/c$  [10]. The unit cell consists of four formula units ( $Z=4$ ) with 40 atoms in all. The site symmetry of Na, M, Si,  $\text{O}_1$ ,  $\text{O}_2$  and  $\text{O}_3$  atoms are (4e), (4e), (8f), (8f), (8f) and (8f), respectively. Thus, the factor-group-analysis (FGA) yields:  $(\text{Na}, \text{M})(C_2) \Gamma = A_g + A_u + 2B_{1g} + 2B_u$ ;  $(\text{Si}, \text{O}_1, \text{O}_2, \text{O}_3)(C_1) \Gamma = 3A_g + 3A_u + 3B_g + 3B_u$ . Summarizing these representations and subtracting the acoustic modes ( $A_u + 2B_u$ ), we obtain the following irreducible representations of  $\text{NaMSi}_2\text{O}_6$  vibrational modes:

$$\begin{aligned} \Gamma_{\text{NaMSi}_2\text{O}_6}^{\text{opt.}} &= 14A_g(xx, yy, zz, xz) + 16B_g(xy, yz) \\ &+ 13A_u(\mathbf{E}||\mathbf{y}) + 14B_u(\mathbf{E}||\mathbf{x}, \mathbf{E}||\mathbf{y}) \end{aligned}$$

The unpolarized Raman spectra of  $\text{NaMSi}_2\text{O}_6$  (M=Ti, V, Cr) are shown in Fig. 2. At the room temperature we find around 30 phonon modes as predicted by FGA. The Raman spectra of different compounds are similar as expected for isostructural materials, and the phonon modes can be crudely grouped into two energy regions. The modes in the spectral range below  $500 \text{ cm}^{-1}$  originate from the bond bending vibrations, whereas the higher frequency modes originate from the stretching vibrations. The highest energy modes are mainly due to the non-bridging Si-O ion vibrations, because

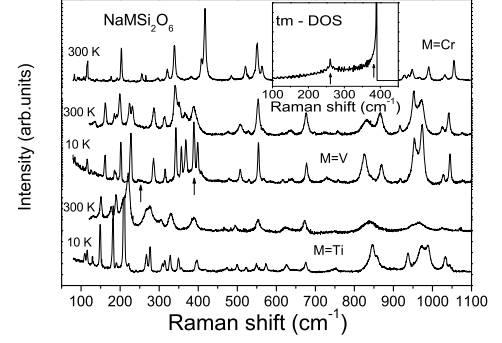


FIG. 2: Raman spectra of  $\text{NaMSi}_2\text{O}_6$ , M=Cr, M=V, and M=Ti. Inset: Two-magnon density of state in  $\text{NaVSi}_2\text{O}_6$ .

of the shortest Si-O tetrahedral bonds. The modes of  $\text{NaMSi}_2\text{O}_6$  at  $1055/1032 \text{ cm}^{-1}$  (Cr),  $1042/1025 \text{ cm}^{-1}$  (V), and  $1042/1025 \text{ cm}^{-1}$  (Ti), represent Si- $\text{O}_2$  (see Fig. 1) antisymmetric/symmetric bond stretching vibrations, respectively. Their frequency difference scales as  $R^{-3}$  in a full accordance with difference between Si- $\text{O}_2$  bond lengths in these materials. Similarly, the modes at  $990/967 \text{ cm}^{-1}$  (Cr),  $972/954 \text{ cm}^{-1}$  (V), and  $965 \text{ cm}^{-1}$  (Ti), we assign as antisymmetric/symmetric pairs of Si- $\text{O}_1$  bond stretching modes. This simplified mode assignment becomes inapplicable at lower frequencies due to more complicated normal coordinates of corresponding vibrations. However, besides similarities, we also observe two very important effects, Fig.2. First, most of the *phonon line widths are dramatically increasing in the components with smaller spin values* ( $V^{3+} \rightarrow S=1$ ,  $\text{Cr}^{3+} \rightarrow S=3/2$ ). Second, the spectra of  $\text{NaTiSi}_2\text{O}_6$ , due to the large phonon broadening, show effectively less phonon modes than expected by FGA, and observed in other pyroxenes. The latter effect may also be regarded as a consequence of a high temperature "higher symmetry lattice state" of  $\text{NaTiSi}_2\text{O}_6$ .

By lowering the temperature, in  $\text{NaTiSi}_2\text{O}_6$  we find a large change in the phonon frequencies and line widths at the phase transition temperature at 210 K. Some typical temperature dependencies of the phonon frequencies are shown in Fig. 3a-c. The mode at about  $946 \text{ cm}^{-1}$  softens by about  $10 \text{ cm}^{-1}$ , while mode at  $966 \text{ cm}^{-1}$  "splits", and hardens by  $25 \text{ cm}^{-1}$ . Existence of the large phonon hardening and softening is a signature of the structural phase transition, which drives the system into the phase with different lattice distortions. The full width at half maximum (FWHM) of the  $946 \text{ cm}^{-1}$  phonon (Lorentzian-fit) increases up to the maximum value at about 210 K, and then decreases to the saturation value which is approximately twice smaller than the  $T=300 \text{ K}$  value, see inset of Fig. 3. This means that *the bond fluctuations are considerably larger in the high-T than in low-T phase* (proximity of the structural phase transition induces the largest fluctuations, producing the maximum FWHM at  $T_{\text{OO}}$ ). Interestingly, the total number of modes in the low-T phase is the same as predicted by FGA for the reg-

ular high-T phase of pyroxenes. However, several modes change the symmetry below  $T_{OO}$  which was observed from the *anti-crossing behavior* of the phonon frequencies, see Fig. 3a. The modes at 221 and 209  $\text{cm}^{-1}$  in Ti compound have the opposite energy shifts by lowering the temperature. They become the modes with the same symmetry below the phase transition temperature, and the interaction causes the anti-crossing behavior. In the V compound (the corresponding modes are at 225 and 232  $\text{cm}^{-1}$ ), they remain independent of each other (no interaction) in the whole temperature region, see Fig. 3d. A similar effect is observed for all other pairs of modes in the spectra, which suggests that in the low-T phase of  $\text{NaTiSi}_2\text{O}_6$  all Raman active modes have the  $A_g$  symmetry. Furthermore, our reflectance measurements (will be published separately, Ref. [11]) show that the infrared active phonon modes can be distinguished from the Raman modes, since the center of inversion remains to be the symmetry element in the low-T phase. Accordingly, we uniquely determine the space group of the low-T phase of  $\text{NaTiSi}_2\text{O}_6$  to be  $P\bar{1}$ . *This space group requires the translation symmetry breaking of the  $\text{TiO}_6$  chain* (the tentative distortion pattern of the low-T phase is shown in Fig. 1) which is in agreement with preliminary X-ray diffraction and neutron scattering data [12].

Contrary to  $S=1/2$  compound, in the low temperature Raman spectra of  $\text{NaVSi}_2\text{O}_6$ , see Fig. 2, and Fig. 3, we did not observe the phonon anomalies. Instead, at temperatures below 19 K, broad asymmetric features, typical for the two-magnon excitations in Heisenberg AF ( $H = \sum_{i,j} J_{i,j} \mathbf{S}_i \cdot \mathbf{S}_j, J_{i,j} > 0$ ), appear around 260 and 400  $\text{cm}^{-1}$ . According to the linear Anderson's approximation, differential cross section for the two-magnon (tm) Raman scattering is proportional to the two-magnon density of states (DOS),  $I_{tm} \sim \sum_{\mathbf{k}} \delta(\omega - 2\omega(\mathbf{k}))$ . The dispersion relation is obtained assuming two-dimensional magnetic structure with different exchange interactions along the chains ( $J_{\parallel}$ ), and perpendicular ( $J_{\perp}$ ) to the chains:  $\omega(\mathbf{k}) = 2S\sqrt{(J_{\parallel} + J_{\perp})^2 - (J_{\parallel}\cos(ka) + J_{\perp}\cos(kb))^2}$ . The calculated two-magnon DOS is shown in Inset of Fig. 2. Two singularities at energies of about 260 and 390  $\text{cm}^{-1}$  are obtained for  $J_{\parallel} = 85$  and  $J_{\perp} = 13 \text{ cm}^{-1}$  (120 K and 18 K, respectively), in a very good agreement with experiment. The maximum of the susceptibility curve in  $\text{NaVSi}_2\text{O}_6$  is at about 100 K [13] which is in excellent agreement with our estimation of the  $J_{\parallel}$ . Thus, we conclude that *the phase transition at about  $T_N=19 \text{ K}$  in  $\text{NaVSi}_2\text{O}_6$  corresponds to the N el-type AF phase transition*. Similar AF phase transitions have been already observed in other  $S=1$  chain compounds  $\text{LiVGe}_2\text{O}_6$  [7], and  $\text{NaVGe}_2\text{O}_6$  [9].

*Pyroxenes: theoretical.* In the following, we discuss the electronic structure of pyroxenes and derive a microscopic model for the orbital and spin degrees of freedom. For a single octahedron the cubic crystal field splits the Ti, V or Cr 3d-states into low lying  $t_{2g}$  states, with 1, 2 or 3 electrons, respectively, and empty states of  $e_g$  symmetry

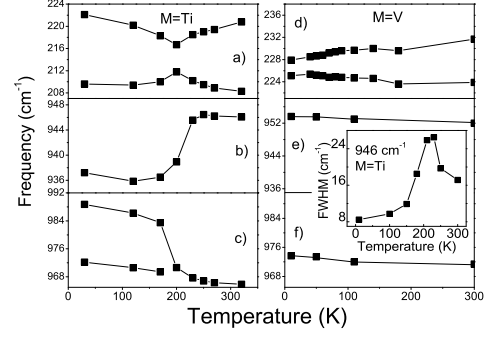


FIG. 3: Temperature dependence of the phonon frequencies in  $\text{NaTiSi}_2\text{O}_6$ , and  $\text{NaVSi}_2\text{O}_6$ . Inset: Temperature dependence of the line width of 946  $\text{cm}^{-1}$  mode.

at higher energy. The low energy electronic properties are governed by the three-fold degenerate  $t_{2g}$  states (the relevant states are  $|xy\rangle$ ,  $|yz\rangle$  and  $|zx\rangle$ ) [14]. The Coulomb interaction  $U$  between electrons on the same transition metal atoms is large, so the exchange interactions can be determined by a second order perturbation expansion in the electron hopping parameters. The problem is further reduced by considering the symmetry allowed hopping paths in the chain geometry, schematically represented in Fig. 4. If we consider orbitals on two sites in the same  $xy$  plane, then only the hopping between  $|xy\rangle$  orbitals is relevant (see Fig. 4a). For sites in the  $yz$  plane, the  $|yz\rangle$  orbitals are relevant, Fig. 4b. In the present geometry (note that x, y, and z in Fig. 4 do not correspond to a, b, and c axis in Fig. 1) there are no transition metal atoms in the same chain that are also in the same  $xz$  plane. The  $|xz\rangle$  orbitals are therefore non-bonding and can be considered inert on this level of approximation (a tightbinding parametrization [15] shows that other overlap integrals either vanish by symmetry or are more than factor five smaller), see Fig. 4c. For the  $S=1/2$  Titanium system we then obtain the Hamiltonian [16],

$$H^{\text{Ti}} = |J^{\text{Ti}}| \sum_{i,j} \mathbf{S}_i \cdot \mathbf{S}_j \left[ \frac{1}{4} T_i^z T_j^z + \frac{(-1)^i}{2} (T_i^z + T_j^z) \right], \quad (1)$$

where we use the orbital operators  $T$  ( $T_i^z = 1/2$  corresponds to an occupied  $|xy\rangle$  orbital and  $T_i^z = -1/2$  to an occupied  $|yz\rangle$  orbital on site  $i$ ), and  $i, j$  are neighboring sites. For the  $S=1$  Vanadium and  $S=3/2$  Chromium system the orbital degree of freedom vanishes ( $T = 0$ ) as the both of the *active* orbitals are occupied, so for the spin system we obtain a simple Heisenberg Hamiltonian  $H^{\text{V/Cr}} = |J^{\text{V/Cr}}| \sum_{i,j} \mathbf{S}_i \cdot \mathbf{S}_j$ . This immediately explains the AF behaviour that is found in all  $S \neq 1/2$  pyroxenes.

*Interpretation of experiments.* The ground state of Hamiltonian (1), is clearly a *ferro-orbital* state, with spin-singlets on each bond, where the energy per dimer is  $-3J^{\text{Ti}}/4$ . The state with all  $|xy\rangle$  occupied is degenerate with the state with all  $|yz\rangle$  occupied, see Fig. 4. Those states do differ, however, because the dimerization pattern along the chain is shifted by one lattice spacing.

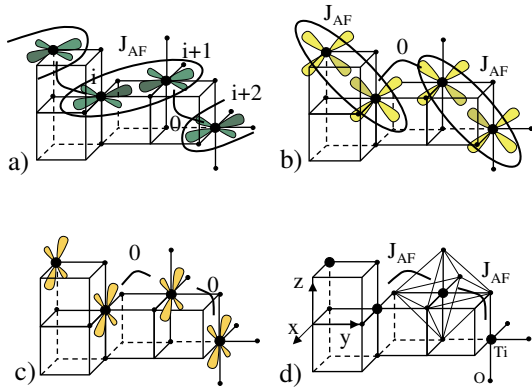


FIG. 4: Schematic presentation of the orbital ordering in  $\text{NaTiSi}_2\text{O}_6$ . Orbital overlap in a) xy, b) yz, and c) xz planes. d) Heisenberg AF phase.

At zero temperature the system is condensed in either one of these two dimerized orbital ordered states and the translation symmetry is broken. This explains the observation of a large spin gap in the susceptibility measurements [6], the symmetry change and the energy shifts of the phonon excitations in the Raman spectra, and the low-temperature structural data [12].

The AF spin fluctuations above the orbital ordering temperature [6] can be easily understood in a straightforward mean-field approximation of Hamiltonian (1), where we can decouple orbitals and spins. If the long range order is absent in the orbital sector, we have for the expectation values  $\langle T_i^z \rangle = 0$ , and  $|\langle T_i^z T_j^z \rangle| < 1/4$ , so that the effective exchange constants –and therefore the fluctuations in the spin-sector– are still antiferromagnetic. Thus, the nature of the phase transition in  $\text{NaTiSi}_2\text{O}_6$  can be established: it corresponds to an orbital order-disorder phase transition with appropriate concomitant magnetic and lattice changes.

One has to keep in mind that the structural changes go hand in hand with the orbital ordering in this compound. Above  $T_{\text{OO}}$  the JT distortion disappears: the high-T orbital disordered phase of  $\text{NaTiSi}_2\text{O}_6$  may be

regarded as an orbital fluctuating phase, and on larger time scales the  $\text{TiO}_6$  octahedra appear to be undistorted. This causes the crystal to be effectively more symmetric, which is in agreement with the observation of less-than-expected phonon modes in the room temperature Raman spectra. But such fluctuations induce large phonon broadenings (of course, the modes with Ti-O bonds in their normal coordinates will be mostly affected), as they are also found in the room temperature Raman spectra of  $\text{NaTiSi}_2\text{O}_6$ , see Fig. 2. In that respect the high-T phase of  $\text{NaTiSi}_2\text{O}_6$  resembles a *dynamical JT phase* (where the phonon broadening is a signature of the melted static lattice distortions [17, 18]).

In the case of two electrons per site ( $\text{NaVSi}_2\text{O}_6$ ), the orbital fluctuations are strongly suppressed due to inert property of  $|xz\rangle$  orbitals, and the corresponding phonon broadenings are much smaller, see Fig. 2.  $\text{NaCrSi}_2\text{O}_6$  has a fully polarized  $t_{2g}$  core, no orbital degrees of freedom, and no anomalous phonon broadenings in the Raman spectra, see Fig. 2.

*Conclusions.* We report a study of the two types of the phase transitions, observed in pyroxene family, by analyzing the Raman-active phonon and magnon excitations, and their temperature dependence. We find that spin  $S=1/2$  compound,  $\text{NaTiSi}_2\text{O}_6$ , exhibits a transition at about 210 K that we assign to be an orbital order-disorder phase transition. It originates from the instability of the high temperature orbital fluctuating - dynamical Jahn-Teller phase, towards a dimerized orbital ordered state, which is accompanied by a lattice distortion and by spin valence bond formation. The spin  $S=1$  system,  $\text{NaVSi}_2\text{O}_6$ , on the contrary, does not show this type of instability and orders as a Néel-type antiferromagnet below  $T_N = 19$  K in agreement with our microscopic spin-orbital model for the pyroxenes.

M.J.K. and Z.V.P. acknowledge support from the Research Council of the K.U. Leuven and DWTC. The work at the K.U. Leuven is supported by Belgian IUAP and Flemish FWO and GOA Programs.

\*milan.konstantinovic@fys.kuleuven.ac.be

- 
- [1] M. Imada, A. Fujimori, and Y. Tokura, Rev. Mod. Phys. **40**, 1039 (1998); Y. Tokura and N. Nagaosa, Science **288**, 462 (2000).
  - [2] K. I. Kugel and D. I. Khomskii, Sov. Phys. JETP **37**, 725 (1973); Sov. Phys. Usp. **25**, 232 (1982).
  - [3] B. Keimer, et al. Phys. Rev. Lett. **85**, 3946 (2000); G. Khaliullin and S. Maekawa, *ibid.* **85**, 3950 (2000).
  - [4] C. Castellani, C. R. Natoli, and J. Ranninger, Phys. Rev. B **18**, 4945 (1978).
  - [5] H.F. Pen, et al. Phys. Rev. Lett. **78**, 1323 (1997).
  - [6] M. Isobe, et al., J. Phys. Soc. Japan. **71**, 1423 (2002).
  - [7] M. D. Lumsden, et al., Phys. Rev. B. **62**, R9244 (2000).
  - [8] P. Vonlanthen, et al., Phys. Rev. B **65**, 214413 (2002).
  - [9] A. N. Vasiliev, et al., JETP Letters **76**, 35 (2002).
  - [10] H. Ohashi, T. Fujita, and T. Osawa, J. Jpn. Assoc. Mineral. Petrol. Econ. Geol. **77**, 305 (1982).
  - [11] Z. V. Popović et.al. in preparation.
  - [12] E. Ninomiya, et al., Proceeding issue of LT23, Japan, 2002.
  - [13] M. Isobe et al., unpublished.
  - [14] The splitting of  $t_{2g}$ 's due to non-cubic crystal fields is generally weak and smaller than typical hopping integrals.
  - [15] W. A. Harrison, Electronic Structure and Properties of Solids, Freeman, San Francisco (1980).
  - [16] We neglect the weak ferromagnetism that results from the Hund's rule exchange.
  - [17] V. Dediu, et al., Phys. Rev. Lett. **84**, 4489 (2000).
  - [18] L. Martín-Carrón and A. de Andres, Eur. Phys. J. B **22**, 11 (2001).